

MedVH: Towards Systematic Evaluation of Hallucination for Large Vision Language Models in the Medical Context

Anonymous ACL submission

Abstract

Large Vision Language Models (LVLMs) have recently achieved superior performance in various tasks on natural image and text data, which inspires a large amount of studies for LVLMs fine-tuning and training. Despite their advancements, there has been scant research on the robustness of these models against hallucination when fine-tuned on smaller datasets. In this study, we introduce a new benchmark dataset, the Medical Visual Hallucination Test (MedVH), to evaluate the hallucination of domain-specific LVLMs. MedVH comprises five tasks to evaluate hallucinations in LVLMs within the medical context, which includes tasks for comprehensive understanding of textual and visual input, as well as long textual response generation. Our extensive experiments with both general and medical LVLMs reveal that, although medical LVLMs demonstrate promising performance on standard medical tasks, they are particularly susceptible to hallucinations, often more so than the general models, raising significant concerns about the reliability of these domain-specific models. For medical LVLMs to be truly valuable in real-world applications, they must not only accurately integrate medical knowledge but also maintain robust reasoning abilities to prevent hallucination. Our work paves the way for future evaluations of these studies.¹

1 Introduction

Recent advancements in large language models (LLMs) have stimulated the development of domain-specific LLM applications in various sectors (Fu et al., 2024; Tran et al., 2024; Bayer et al., 2024), including healthcare (Singhal et al., 2023). Building on this, researchers have further introduced large vision language models (LVLMs) that combine the robust capabilities of LLMs with the

processing of visual inputs (Li et al., 2023b; Liu et al., 2023). However, despite the promising performance, both LLMs and LVLMs encounter this critical issue known as “hallucination”, where they produce seemingly correct yet unverified responses with great confidence (Bang et al., 2023; Liu et al., 2024). Numerous studies have been trying to identify, evaluate, and mitigate the occurrence of hallucinations of large-scale models (Wu et al., 2024; Manakul et al., 2023; Shuster et al., 2021; Li et al., 2023c; Ye et al., 2023).

However, despite the recent emergence of medically specialized LVLMs (Moor et al., 2023; Li et al., 2023a), research specifically targeting hallucinations in the medical context remains limited. On the one hand, the fine-tuning of LVLMs for domain-specific tasks, such as interpreting chest X-ray images, has demonstrated significant performance improvements (Lee et al., 2024; Chen et al., 2024). These advances suggest the potential for a more accessible image analysis system that could not only empower patients with vital information about their health conditions but also provide physicians with a reliable second opinion to support more informed clinical decisions. On the other hand, the susceptibility of these systems to hallucinations poses a serious risk, potentially leading to adverse effects on healthcare decisions, diagnoses, and treatment plans. Developing a test to assess this would necessitate extensive domain expertise and the creation of specifically curated input data, such as images with hard negative diagnostic results. This underscores the urgent need for focused research to evaluate and enhance the robustness and proficiency of medical LVLMs.

This paper aims to bridge this gap by introducing a novel benchmark dataset, Medical Visual Hallucination Test (MedVH), to evaluate LVLMs’ capabilities in dealing with hallucinations in the medical context from two facets. We demonstrate the overall evaluation framework in Figure 1 and

¹Our dataset is available at <https://anonymous.4open.science/r/MedVH-01B7>

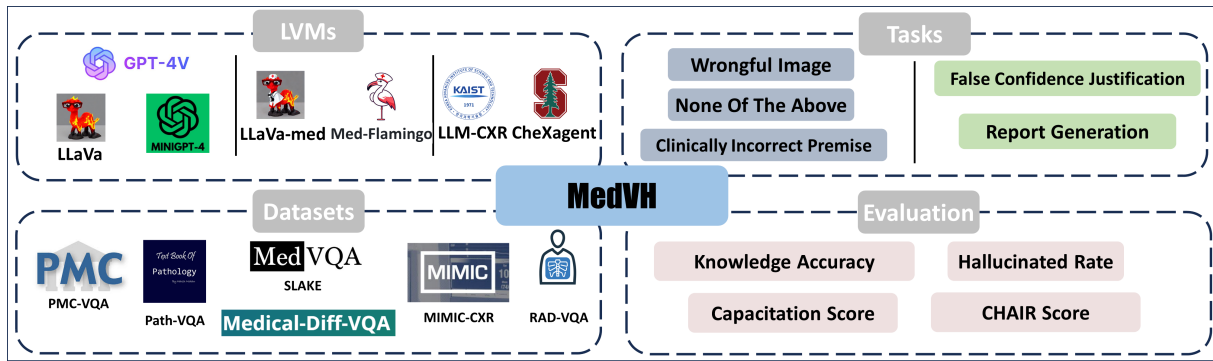


Figure 1: Overall evaluation framework.

081 a comparison of MedVH with the existing hallucination benchmark datasets in Table 1. We first
 082 examine the model’s capability of comprehensive
 083 understanding of both visual information and textual input. Following Umaphathi et al. (2023), we
 084 conduct our test through multi-choice visual question answering (MC-VQA), with multimodal input
 085 comprising an image, a textual question, and multiple potential answers. These tasks do not require
 086 models to generate long responses, but to consider the information gathered from the image, together
 087 with its own medical knowledge, and the input textual information. The difficulties lie in distinguishing
 088 correct medical findings from misleading inputs that could lead to hallucinations, such as unrelated
 089 images or clinically incorrect premises in the questions. Furthermore, we also examine the models’
 090 capability to resist the lure to hallucinate when they generate long textual responses. As noted by
 091 Yifan Li and Wen (2023), hallucinations can stem from the high likelihood of co-occurring
 092 objects, which, in a medical setting, might become co-appearing medical terms or diagnoses. Imaginably,
 093 the longer the generated content, the more likely it will fall into the pitfall of probabilities. We
 094 conduct this test with medical report generation and false confidence justification with MC-VQA,
 095 both requiring long responses.

096 In this work, we focus on the visual task related to the chest X-ray (CXR) images, which is one of the most studied medical imaging domains (Çalli et al., 2021; Al-Waisy et al., 2023; Alshmrani et al., 2023). As shown in Figure 1, we construct the novel MC-VQA benchmark dataset by synthesizing a line of publicly available datasets, including RAD-VQA (Lau et al., 2018), SLAKE (Liu et al., 2021), PMC-VQA (Zhang et al., 2023), Path-VQA (He et al., 2020), VQA-Med-2021 (Ben Abacha et al., 2021), and MIMIC-Diff-VQA (Hu et al., 2023), while the report gener-

121 ation input samples are randomly drawn from
 122 MIMIC-CXR. We conduct experiments with three
 123 types LVMs: general models (ChatGPT-4V²,
 124 MiniGPT (Chen et al., 2023), LLaVA (Liu et al.,
 125 2023a), Med-Flamingo (Moor et al., 2023)), and
 126 CXR fine-tuned LVMs (CheXAgent (Chen et al.,
 127 2024), LLM-CXR (Lee et al., 2024)). Experimental
 128 results reveal that, despite the improved per-
 129 formance of domain-specific fine-tuned LVMs in
 130 standard medical tasks, they are even more suscep-
 131 tible to hallucinations compared to the models in
 132 the general domain, raising serious concerns about
 133 the reliability of these fine-tuned models in med-
 134 ical applications. Through this study, we aim to
 135 contribute to the development of more reliable and
 136 trustworthy language models within the medical
 137 context and promote the practical application of
 138 such AI models in real-life healthcare scenarios.

139 The contributions of our study are outlined as
 140 follows:
 141

- 142 • We construct the first benchmark dataset for
 143 evaluating the hallucination of LVMs in the
 144 medical context, which evaluates medical vi-
 145 sual hallucination through textual-visual un-
 146 derstanding and long text generation.
- 147 • We propose to evaluate LVMs with five di-
 148 verse domain-specific tasks, and a characteri-
 149 zation evaluation metric measuring the com-
 150 bined capability of reasoning and utilization
 151 of medical knowledge.
- 152 • We perform comprehensive experiments with
 153 three types, seven in total state-of-the-art
 154 LVMs, revealing the lack of robustness of ex-
 155 isting domain-specific fine-tuned expert mod-
 156 els, indicating space for improvement before
 157 further integration in real-life applications.

²<https://openai.com/index/gpt-4/>

	Multimodality	Medical Knowledge Test	Diagnosis Level Test	Question Type
CHAIR	✓	✗	✗	Open
POPE	✓	✗	✗	MC
MME	✓	✗	✗	MC
Med-Halt	✗	✓	✗	MC/Open
<i>SourceCheckup</i>	✗	✓	✗	Open
MedVH	✓	✓	✓	MC/Open

Table 1: Comparison with existing hallucination benchmarks. *Open* stands for opentext generation. *MC* stands multi-choice question answering.

2 Related Work

With the advent of LLMs, researchers have advanced to developing multimodal large-scale models, or LVLMs (Liu et al., 2023; Chen et al., 2023). Several efforts have also been made to adapt such LVLMs for use in the medical field, such as LLaVA-med (Li et al., 2023a) and CheX-agent (Chen et al., 2024). However, numerous efforts have highlighted the risk of hallucinations in large models, casting doubt on their reliability in critical fields such as healthcare. Mündler et al. (2024) have identified and suggested methods to address self-contradiction in LLMs. Umapathi et al. (2023) introduced Med-Halt to assess reasoning and memory-based hallucinations with medical entrance exams, finding that no model achieved satisfactory accuracy across most tasks. Yifan Li and Wen (2023) developed POPE to evaluate visual hallucinations in object detection in general images, noting LVLMs often identify objects that frequently appear or co-occur in their training datasets. Despite these efforts, research into hallucinations in medical vision-language tasks is still limited.

3 Hallucination Evaluation

In this section, we introduce our evaluation framework for assessing hallucinations in LVLMs within the medical domain. The overview of this framework is illustrated in Figure 1. We have developed a new benchmark dataset, MedVH, designed to evaluate the models across two distinct facets through five tasks that probe key functionalities. The following sections will offer a detailed explanation of the framework, the tasks associated with each facet of evaluation, and the metrics used for assessment.

3.1 Overall Evaluation Framework

As demonstrated in Figure 1, we evaluate seven state-of-the-art LVLMs from two facets, each corresponding to a different type of hallucination in the medical context. The first facet examines the models’ robustness against hallucinations in comprehensive understanding of medical visual informa-

tion and textual input through MC-VQA tasks, such as disease identification and severity assessment. The second facet focuses on hallucinations occurring in long text generation, particularly with false confidence justification and medical report generation. We detail each task within the MedVH dataset in Figure 2, and provide examples of prompts used in these tasks in Figure 9 of Appendix E. The models’ robustness against hallucinations will be evaluated considering their ability to leverage the medical knowledge base and their model size.

3.2 Medical Visual and Text Understanding

We begin by assessing the presence of hallucinations in LVLMs with visual and textual comprehension. Specifically, we evaluate the models’ capability to discern irrelevant or incorrect inputs and detect misleading instructions. To achieve this, we introduce three MC-VQA tasks, which involves multi-modal input comprising both an image and a textual question. The models are tested in the following settings.

Wrongful Image This task is designed to evaluate the model’s capability to recognize inconsistencies between the image content and the associated question, in which we replace the corresponding images with unrelated ones. We either randomly select a wrongful medical image from a different genre or choose an adversarial X-ray image of a different organ. For instance, in the task of disease identification using chest X-ray images, a randomly chosen image could be a retinal image or a picture of cells, while an adversarial image would be an X-ray image of another organ that does not exhibit the targeted disease.

None Of The Above In this task, models are presented with a multi-choice question where the correct answer is explicitly listed as ‘None of the above’. This setup requires the model to recognize and select this option, effectively testing its ability to discern irrelevant or incorrect options presented in the choices.

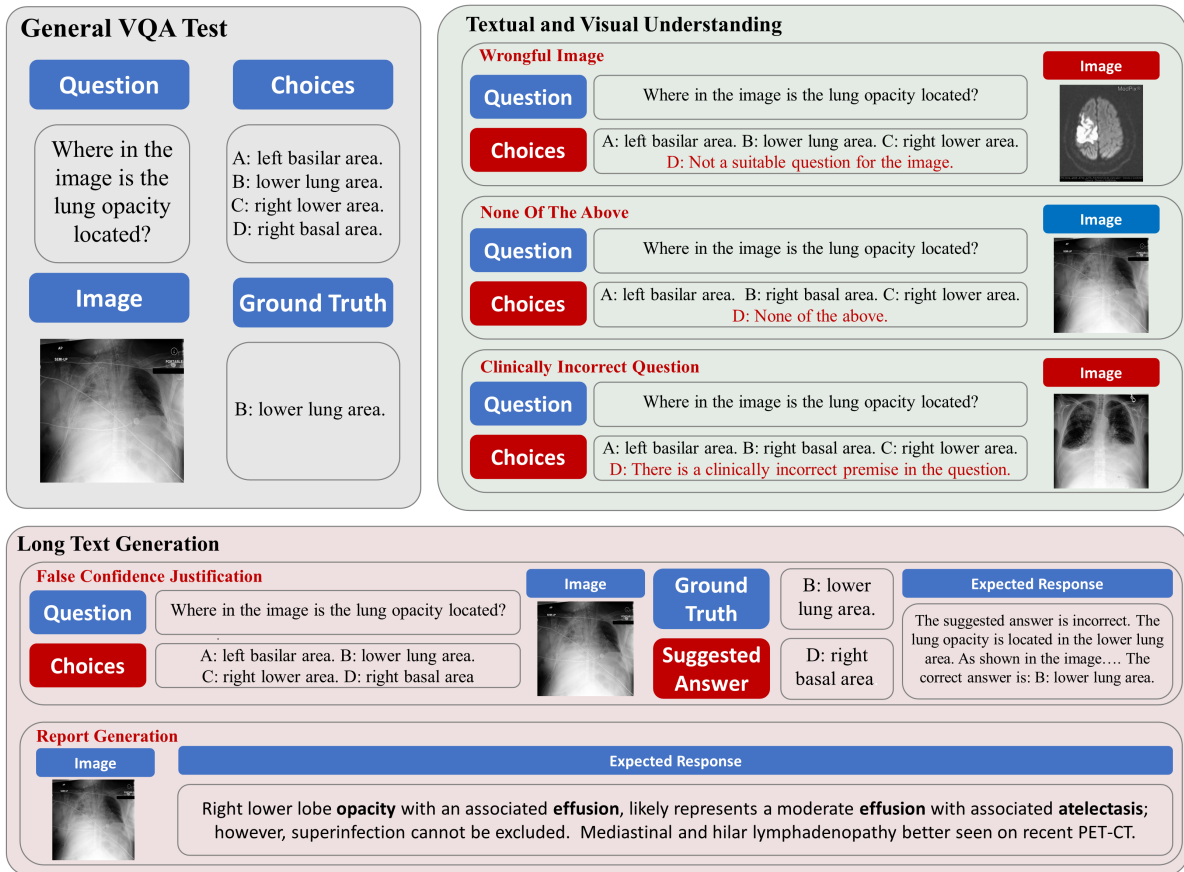


Figure 2: Detailed illustration of evaluation tasks in MedVH.

Clinically Incorrect Questions This task assesses the ability of LVLMs to correctly align the specific clinical findings visible in images with the descriptions provided in the questions. In this scenario, the proposed question inquires about a specific feature that, contrary to what is suggested, does not appear in the corresponding image. This task not only tests the model’s capability for interpreting medical images with domain-specific knowledge but also demands a strong reasoning ability to identify the contradiction.

3.3 Medical Text Generation

We also evaluate the appearance of hallucination in the long textual response of the LVLMs under the following two settings.

False Confidence Justification This task presents a question and a randomly suggested wrong answer to the language model, and then asks the model to provide detailed explanations for its correctness or incorrectness. The model is supposed to suggest an alternative answer if it decides the suggested answer is incorrect. This test specifically examines the language model’s propensity to express answers with unwarranted

certainty in the input text.

General Report Generation In this task, we prompt the LVLMs to generate medical reports based on CXR images. The objective is for the models to accurately identify diseases visible in the image. Any mention of diseases not present in the image will be considered a hallucination. This setup evaluates the models’ precision in recognizing and reporting medical conditions from visual inputs while generating long textual responses.

3.4 Data Synthesis and Statistics

For each of the MC-VQA tasks and the False Confidence Justification task with multi-choice questions, we establish our benchmark by randomly sampling 500 questions from four publicly available medical VQA datasets: RAD-VQA, SLAKE, PMC-VQA, and MIMIC-Diff-VQA. As for the unrelated medical images and adversarial X-ray images in the Wrongful Image task, we randomly select the images Path-VQA and Med-VQA-2021 respectively. Among these datasets, RAD-VQA, SLAKE, and PMC-VQA mainly focus on medical knowledge-based questions, with only a small portion of general diagnosis-level questions like “What is abnormal about the lung?”. On the other hand,

MIMIC-Diff-VQA, derived from de-identified patient data in MIMIC-CXR, includes a larger proportion of specific diagnostic-level questions, like “Where in the image is the pleural effusion located?” The details and statistics of these datasets are presented in Table 4 of subsection C.1.

Except for PMC-VQA, the other three datasets do not provide options for each question. For MedVH, we therefore generate answer choices for the MC-VQA questions by randomly sampling from the answers associated with the same questions. In this manner, all the datasets would be eligible being the source of the Wrongful Image task and the False Confidence Justification task. However, due to the limited number of repeated questions in RAD-VQA and SLAKE, excluding the ground truth answer to create a None Of The Above option would often leave only one plausible answer, reducing it to a true-or-false question. In this case, only PMC-VQA and MIMIC-Diff-VQA are utilized in the None Of The Above task. Similarly, due to the limited availability of diagnosis-level questions and the absence of hard-negative images related to the specified diseases, only MIMIC-Diff-VQA is included in the Clinically Incorrect Question task. We demonstrate the distribution of question sources in Figure 8 of subsection C.1. As for the medical report generation, we randomly sampled 200 CXR images from MIMIC-CXR.

3.5 Evaluation

Multi-choice VQA. For each multi-choice question, there is a designated correct answer. We quantify the model’s success rate in selecting this answer using the metric acc_h . A higher acc_h score indicates greater resistance of the model to hallucinations. Additionally, we also assess the model’s performance on regular MC-VQA tasks as baseline experiments, which involve standard CXR images, correct answers among the options, and questions based on accurate clinical assumptions, serving to evaluate the model’s medical knowledge. We represent the models’ accuracy on this baseline task with acc_b . Ideally, an LVM should demonstrate both a broad medical knowledge base and the ability to generate responses free from hallucinations.

Characterization score. In this study, we introduce the characterization score as a comprehensive evaluation metric, which is designed to effectively balance the requirements of robustness against hallucinations with the accuracy of medical knowledge. Analogous to the way precision and recall

are combined in the Micro-F1 metric, the characterization score, $char_score$, is calculated as the weighted harmonic mean of acc_h and acc_b :

$$char_score = \frac{w_h + w_b}{\frac{w_h}{acc_h} + \frac{w_b}{acc_b}} = \frac{(w_h + w_b) \times acc_h \times acc_b}{w_h \times acc_h + w_b \times acc_b},$$

where $w_h, w_b \in [0, 1]$ are weights for hallucination test accuracy acc_h and baseline test accuracy acc_b respectively, satisfying $w_h + w_b = 1$. Naturally, the characterization score, with assigned equal weights to acc_h and acc_b , typically exhibits a low value when either of these scores is low, as demonstrated in Figure 7 within Appendix A. This observation underscores the significant concurrent dependence of the characterization score on both metrics. Moreover, the weights can be tailored to suit the specific requirements of different applications, allowing for flexibility in adapting the model to varied use cases. **False Confidence Justification.** For evaluation, we will measure the propensity of LVMs to disagree with a suggested incorrect answer, denoted as $r_{disagree}$. Additionally, we will calculate $r_{correct}$, the ratio indicating how often the alternative answer proposed by the LVMs is correct. We will also establish a baseline, $r_{baseline}$, which represents the accuracy of the LVMs when responding to the same set of questions without any suggested incorrect answers.

General Report Generation. We incorporate CHAIR(Rohrbach et al., 2018) to calculate the proportion of diseases that appear in the report but not the CXR image. Specifically, we utilize CheXpert(Irvin et al., 2019) to label the generated reports, and measure both instance-level hallucination $CHAIR_I$ and the sentence-level hallucination $CHAIR_S$ as defined in the following equations:

$$CHAIR_I = \frac{|\{\text{hallucinated diseases}\}|}{|\{\text{all mentioned diseases}\}|},$$

$$CHAIR_S = \frac{|\{\text{sentences with hallucinated diseases}\}|}{|\{\text{all sentences}\}|}.$$

4 Main Results

4.1 Visual and Textual Cross-understanding

We visualize the evaluation results of the *Medical Visual and Text Understanding* test in the left plots of Figure 3, which includes three MC-VQA tasks along with their averaged performance in the sub-plots. Additionally, the numeric results are detailed in Table 5 of Section D. It is observed that CheX-agent excels in the baseline test—where the input

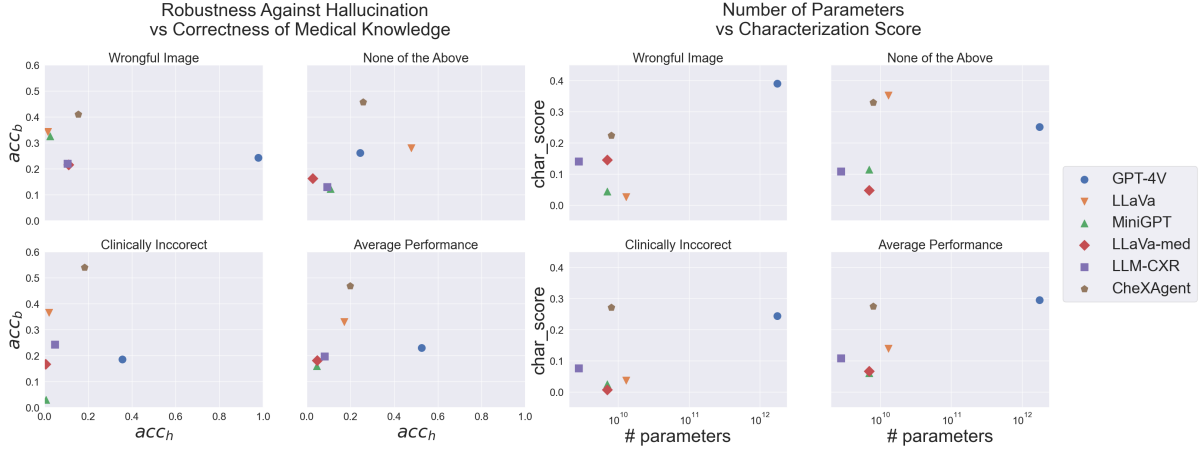


Figure 3: Results on MedVH dataset. (left) Accuracy of hallucination VQA tasks compared with accuracy of regular MC-VQA tasks. (right) Performance on characterization score considering the model size.

	Wrong Suggested Answer		Correct Suggested Answer		No Suggested Answer
	$r_{disagree}$	$r_{correct}$	$r_{disagree}$	$r_{correct}$	
LVLm			$r_{disagree}$	$r_{correct}$	$r_{baseline}$
GPT-4V	0.746	0.366	0.534	0.466	0.378
LLaVa	0.562	0.250	0.504	0.496	0.360
MiniGPT	0.938	0.490	0.950	0.050	0.326
LLaVa-Med	0.308	0.172	0.540	0.460	0.244
LLM-CXR	0.376	0.220	0.310	0.690	0.256
CheXAgent	0.964	0.094	0.768	0.232	0.462

Table 2: Performance on False Confidence Justification. We suggest the incorrect answer to the model in the first two columns. For baselines, we suggest the correct answer to the model in the middle two columns, and do not suggest an answer in the prompt in the last column. We highlight the highest accuracy in each scenario.

image accurately matches the question and the correct answer is provided among the options—yet it lacks robustness when faced with inputs that could lead to hallucination. In contrast, Chat-GPT4V exhibits the most robustness against misleading inputs but falls short in displaying medical knowledge, particularly for diagnosis-level queries in the Clinically Incorrect Question task. It shows exceptional performance in handling wrongful images, likely because this task primarily tests the model’s ability to differentiate between images of various organs and modalities, which demands minimal medical knowledge. The overall characterization scores of the LVLms are also evaluated against their model size. The right plot of Figure 3 shows that CheXAgent, despite having a smaller parameter size, performs comparably to ChatGPT-4V by achieving higher scores in both the None Of The Above and Clinically Incorrect Question tasks.

As for the rest of the models, LLaVa appears somewhere in the middle of CheXAgent and ChatGPT-4V in terms of average performance (left subplot) and third in characterization score (right subplot). This is attributed to its strong perfor-

mance in the None Of The Above task, a result of its propensity to select “None of the above”. This behavior will be discussed further in Section E. Although LLaVa achieves the second highest acc_b scores in all tasks, this is primarily due to its tendency to ignore distractor options such as “This is not a suitable question for the image”, opting instead for a random choice among the remaining options. In contrast, models like MiniGPT find all options equally reasonable due to a lack of medical knowledge. Both LLaVa-Med and LLM-CXR also fail to show competitive performance, underscoring that instruction tuning based solely on general medical knowledge, or a limited amount of tasks and fine-tuning data, does not just compromise robustness against hallucination but also fails to establish a solid medical knowledge base. Note that we exclude the performance of Med-Flamingo from this analysis, as it cannot process MC-VQA tasks in a zero-shot setting, and its performance under the few-shot learning is highly dependent on the provided content, which could be unfair competition for the other models.

	CHAIR _I	CHAIR _S	F ₁
GPT-4V	0.665	0.107	0.338
LLaVa	0.760	0.001	0.194
MiniGPT	0.938	0.149	0.040
LLaVa-med	0.737	0.293	0.218
Med-Flamingo	0.831	0.695	0.133
LLM-CXR	0.570	0.362	0.401
CheXagent	0.461	0.252	0.506

Table 3: Performance on report generation.

4.2 Long Text Generation

We present the models’ performance on the False Confidence Justification in Table 2. CheXagent once again showcases the most reliable medical knowledge base in baseline experiments of the False Confidence Justification task without suggested answers. However, it exhibits a significantly higher tendency to disagree when an answer is suggested. Notably, the probability of disagreement drops when the correct answer is suggested, indicating that it can recognize the correct answer to a certain degree. MiniGPT also shows a consistent pattern of disagreement across all suggested answers, but with no reduction in disagreement when the correct answer is provided. This performance, coupled with an incompatible $r_{baseline}$, indicates a lack of both medical knowledge and reasoning capabilities. In contrast, LLM-CXR performs optimally when the correct answer is suggested. However, its performance drops with incorrect or no suggested answers, which indicates that it may possess the requisite medical knowledge, but lacks the reasoning capabilities to independently identify the correct answer, possibly due to the limited number of parameters and fine-tuning tasks. Notably, LLaVa-Med displays an even higher propensity to disagree with the correct answer and achieves the lowest scores when no answer is suggested, even falling below LLaVa’s performance. This indicates that its fine-tuning not only failed to develop a coherent medical knowledge base but also impaired its original reasoning abilities.

The performance of the Report Generation task is demonstrated in Table 3. General LVLMs, including chat-GPT4V, fail to achieve meaningful performance with a compatible F1 score, indicating that this is indeed the task that requires the most medical knowledge and domain fine-tuning. On the other hand, since there is no misleading input in this task, CheXagent again outperforms the others, but still has a nearly 50% instance-level hallucination. In the meantime, LLM-CXR can

also generate meaningful reports with a compatible F1 score, but with a much higher CHAIR score.

4.3 Instruction Fine-tuning

Based on our experimental findings, there is still significant potential for improvement in the robustness of LVLMs against hallucinations within the medical domain. Our experiments illustrate a notable trade-off between the reasoning capabilities developed from extensive general-domain training and the specialized knowledge obtained through domain-specific fine-tuning. The reasoning ability of a model is critical for its robustness against inputs that may induce hallucinations. Potential enhancements include increasing the model size and conducting comprehensive training with a wide variety of general images. Additionally, the source and volume of medical training data are crucial factors. Specifically, LLaVA-Med does not demonstrate competitiveness in any task, indicating that reliance solely on general PMC data to capture medical concepts is insufficient. On the other hand, the inclusion of diverse domain-specific training tasks and data sources is vital for enriching the medical knowledge base of LVLMs. This point is exemplified by CheXagent, whose superior performance highlights the benefits of instruction-based fine-tuning in endowing models with the necessary knowledge. However, despite its strong performance in regular medical tasks, CheXagent’s tendency to produce hallucinated outputs poses significant concerns for its deployment in real-life settings. Future research should aim to preserve the model’s reasoning ability throughout the fine-tuning process, thus developing a more reliable expert system.

5 Exploratory Analysis

5.1 Effects of Temperature Parameter

We examine the impact of the hyperparameters, temperature, on model-induced hallucinations. Specifically, we employed the Chat-GPT4V and assessed its performance over various temperature settings on the False Confidence Justification task, which did not provide a suggested answer. The results, depicted in Figure 4, show minimal variation in accuracy across different temperature values. These findings suggest that while temperature adjustments do influence the model’s accuracy, their overall effect is relatively minor, which underscores the importance of other factors in mitigating hallucinations within medical vision language tasks.

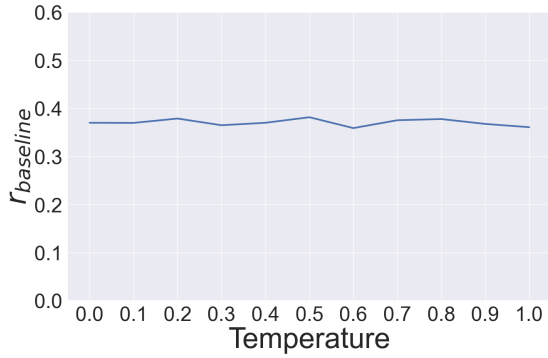


Figure 4: Variation in accuracy for different temperature values of Chat-GPT4V.

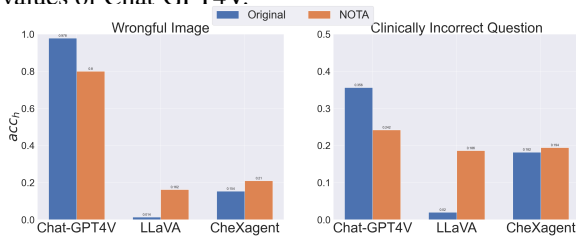


Figure 5: Variation in performance against hallucination for different wording of choices. Original means the ideal extra choice for the question, which should have been “This is not a suitable question for the image” for the Wrongful Image task and “The question contains a clinically incorrect premise” for the Clinically Incorrect Question task, respectively. NOTA indicates we substitute that choice with “None of the above”.

5.2 Sensitivity to Prompt

In Figure 5, we replaced the original options in the Wrongful Image and Clinically Incorrect Question tasks with “None of the above”, which originally were “This is not a suitable question for the image” and “The question contains a clinically incorrect premise”, respectively. As the revised choices are integral to the input textual prompts for these models, our objective is to evaluate LVLMs’ sensitivity to the nuances of prompt wording. Although both the substituted and original options serve to negate the correctness of other available choices, they do not convey the same message. Consequently, the observed decrease in accuracy for Chat-GPT4V is both understandable and anticipated. Conversely, the notable performance improvement in LLaVA once again underscores its propensity to select ‘None of the above’. Additionally, the slight improvement in CheXagent suggests that simpler expressions of incorrectness are more easily interpreted by this model, which also points to a limitation in its reasoning ability.

However, this sensitivity to prompt wording should not be viewed exclusively as a negative attribute. In Figure 6, we incorporated a hint within

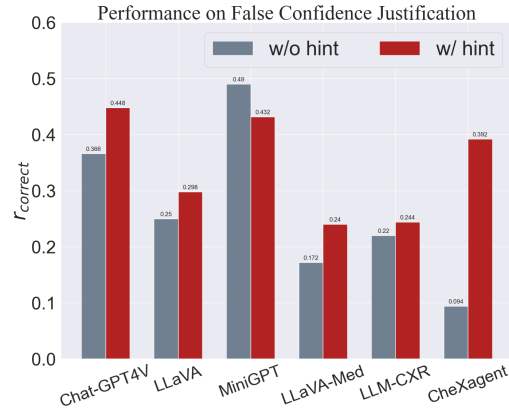


Figure 6: Variation in performance against hallucination for the False Confidence Justification task.

the prompt that suggests the possibility of an incorrect response, which led to improved performance across all models, except MiniGPT. This indicates that careful prompt design can enhance model robustness—a critical aspect in real-world applications involving both patients and physicians. By incorporating user-specific information either in the prompt or even during training, the model can be tailored to handle misleading inputs more effectively. For example, while there is a potential for a patient to upload an incorrect image, the likelihood of such an error by a physician is significantly lower. Acknowledging these user-specific scenarios during model training or in the prompt structure could substantially increase the model’s resilience and accuracy in practical settings.

6 Conclusion

This research investigates hallucination phenomena in domain-specific large vision-language models (LVLMs) after fine-tuning on small datasets. We introduce the MedVH benchmark dataset, which includes five types of tasks designed to evaluate hallucinations, and we compare the performance of both general and medical LVLMs using this dataset. The experimental results indicate that medical LVLMs experience more hallucinations than general LVLMs, despite achieving better performance on standard medical tasks. This inconsistency between hallucination and medical task performance raises significant concerns about the reliability of these domain-specific models, particularly in critical settings like the medical field. By releasing MedVH, we aim to encourage extensive exploration of hallucination tasks in future research, ultimately advancing the development of reliable medical LVLMs.

586 Limitations

587 Despite the comprehension of our proposed bench-
588 mark dataset, there are still some limitations.
589 Firstly, even though our benchmark dataset incorpo-
590 rates multiple public datasets from various sources,
591 there may still be potential for data bias. This is
592 a prevalent challenge in the medical field due to
593 the naturally unbalanced distribution of diagnosis
594 results. Secondly, all datasets used to construct
595 MedVH are publicly available, which may result
596 in an overlap with the training data of some Large
597 Vision-Language Models (LVLMs), such as Chat-
598 GPT, which could affect the fairness and accuracy
599 of our evaluations. Future studies could benefit
600 from assessing these models on a private dataset
601 that more closely mirrors real-world scenarios.

602 Ethics Statement

603 In this study, we introduce an evaluation frame-
604 work for hallucination in Large Vision Language
605 Models (LVLMs) within the medical domain and
606 develop a benchmark dataset. Our framework aims
607 to enhance the understanding of LVLMs' capabil-
608 ities and improve their evaluation prior to imple-
609 mentation in real-world medical applications. We
610 constructed our dataset from multiple publicly ac-
611 cessible sources, including MIMIC-Diff-VQA and
612 MIMIC-CXR. To adhere to the Health Insurance
613 Portability and Accountability Act (HIPAA) stan-
614 dards, all protected health information has been
615 thoroughly anonymized. Consistent with strict pri-
616 vacy protocols, we refrained from directly sharing
617 raw data with the OpenAI API and instead con-
618 ducted our experiments via Azure OpenAI, per the
619 recommendations by PhysioNet³. Furthermore, we
620 will not distribute the raw data from MIMIC-CXR
621 through any unauthorized channels, such as GitHub.
622 The benchmark dataset will be made available on
623 PhysioNet following the publication of this work.

624 References

625 Alaa S Al-Waisy, Shumoos Al-Fahdawi, Mazin Abed
626 Mohammed, Karrar Hameed Abdulkareem,
627 Salama A Mostafa, Mashaal S Maashi, Muham-
628 mad Arif, and Begonya Garcia-Zapirain. 2023.
629 Covid-chexnet: hybrid deep learning framework for
630 identifying covid-19 virus in chest x-rays images.
631 *Soft computing*.

632 Goram Mufarah M. Alshmrani, Qiang Ni, Richard Jiang,
633 Haris Pervaiz, and Nada M. Elshennawy. 2023. A

³<https://physionet.org/news/post/gpt-responsible-use>

deep learning architecture for multi-class lung dis- 634
eases classification using chest x-ray (cxr) images. 635
Alexandria Engineering Journal. 636

Yejin Bang, Samuel Cahyawijaya, Nayeon Lee, Wen- 637
liang Dai, Dan Su, Bryan Wilie, Holy Lovenia, Ziwei 638
Ji, Tiezheng Yu, Willy Chung, Quyet V. Do, Yan Xu, 639
and Pascale Fung. 2023. A multitask, multilingual, 640
multimodal evaluation of ChatGPT on reasoning, hal- 641
lucination, and interactivity. *ACL*. 642

Markus Bayer, Philipp Kuehn, Ramin Shanehsaz, and 643
Christian Reuter. 2024. Cysecbert: A domain- 644
adapted language model for the cybersecurity domain. 645
ACM Transactions on Privacy and Security. 646

Asma Ben Abacha, Mourad Sarrouiti, Dina Demner- 647
Fushman, Sadid A. Hasan, and Henning Müller. 2021. 648
Overview of the vqa-med task at imageclef 2021: Vi- 649
sual question answering and generation in the medi- 650
cal domain. In *CLEF 2021 Working Notes*. 651

Erdi Çallı, Ecem Sogancioglu, Bram van Ginneken, 652
Kicky G van Leeuwen, and Keelin Murphy. 2021. 653
Deep learning for chest x-ray analysis: A survey. 654
Medical Image Analysis. 655

Jun Chen, Deyao Zhu, Xiaoqian Shen, Xiang Li, Zechu 656
Liu, Pengchuan Zhang, Raghuraman Krishnamoor- 657
thi, Vikas Chandra, Yunyang Xiong, and Mohamed 658
Elhoseiny. 2023. Minigpt-v2: large language model 659
as a unified interface for vision-language multi-task 660
learning. *arXiv preprint arXiv: 2310.09478*. 661

Zhihong Chen, Maya Varma, Jean-Benoit Delbrouck, 662
Magdalini Paschali, Louis Blankemeier, Dave Van 663
Veen, Jeya Maria Jose Valanarasu, Alaa Youssef, 664
Joseph Paul Cohen, Eduardo Pontes Reis, Emily B. 665
Tsai, Andrew Johnston, Cameron Olsen, Tan- 666
ishq Mathew Abraham, Sergios Gatidis, Akshay S. 667
Chaudhari, and Curtis Langlotz. 2024. Chexagent: 668
Towards a foundation model for chest x-ray interpre- 669
tation. 670

Weimin Fu, Shijie Li, Yifang Zhao, Haocheng Ma, Raj 671
Dutta, Xuan Zhang, Kaichen Yang, Yier Jin, and 672
Xiaolong Guo. 2024. *Hardware phi-1.5b: A large* 673
language model encodes hardware domain specific 674
knowledge. *Preprint*, arXiv:2402.01728. 675

Xuehai He, Yichen Zhang, Luntian Mou, Eric P. Xing, 676
and Pengtao Xie. 2020. Pathvqa: 30000+ ques- 677
tions for medical visual question answering. *ArXiv*, 678
abs/2003.10286. 679

Xinyue Hu, Lin Gu, Qiyuan An, Mengliang Zhang, 680
Liangchen Liu, Kazuma Kobayashi, Tatsuya Harada, 681
Ronald M. Summers, and Yingying Zhu. 2023. Ex- 682
pert knowledge-aware image difference graph repre- 683
sentation learning for difference-aware medical vi- 684
sual question answering. In *KDD*. 685

Jeremy Irvin, Pranav Rajpurkar, Michael Ko, Yifan Yu, 686
Silviana Ciurea-Ilcus, Chris Chute, Henrik Marklund, 687
Behzad Haghgoo, Robyn Ball, Katie Shpanskaya, 688
Jayne Seekins, David A. Mong, Safwan S. Halabi, 689

690	Jesse K. Sandberg, Ricky Jones, David B. Larson,	Kurt Shuster, Spencer Poff, Moya Chen, Douwe Kiela,	743
691	Curtis P. Langlotz, Bhavik N. Patel, Matthew P. Lun-	and Jason Weston. 2021. Retrieval augmentation	744
692	gren, and Andrew Y. Ng. 2019. Chexpert: A large	reduces hallucination in conversation . <i>Preprint</i> ,	745
693	chest radiograph dataset with uncertainty labels and	arXiv:2104.07567.	746
694	expert comparison.		
695	Jason Lau, Soumya Gayen, Asma Ben Abacha, and	Karan Singhal, Shekoofeh Azizi, Tao Tu, Jason	747
696	Dina Demner-Fushman. 2018. A dataset of clini-	Wei, Hyung Chung, Nathan Scales, Ajay Tan-	748
697	cally generated visual questions and answers about	wani, Heather Cole-Lewis, Stephen Pfohl, Perry	749
698	radiology images. <i>Scientific Data</i> .	Payne, Martin Seneviratne, Paul Gamble, Chris Kelly,	750
699	Suhyeon Lee, Won Jun Kim, Jinho Chang, and	Abubakr Babiker, Nathanael Schärli, Aakanksha	751
700	Jong Chul Ye. 2024. LLM-CXR: Instruction-	Chowdhery, Philip Mansfield, Dina Demner-	752
701	finetuned LLM for CXR image understanding and	Fushman, and Vivek Natarajan. 2023. Large lan-	753
702	generation. In <i>ICLR</i> .	guage models encode clinical knowledge. <i>Nature</i> .	754
703	Chunyuan Li, Cliff Wong, Sheng Zhang, Naoto	Hieu Tran, Zhichao Yang, Zonghai Yao, and Hong Yu.	755
704	Usuyama, Haotian Liu, Jianwei Yang, Tristan Nau-	2024. BioInstruct: instruction tuning of large lan-	756
705	mann, Hoifung Poon, and Jianfeng Gao. 2023a.	guage models for biomedical natural language pro-	757
706	Llava-med: Training a large language-and-vision as-	cessing. <i>Journal of the American Medical Informat-</i>	758
707	sistant for biomedicine in one day.	<i>ics Association</i> .	759
708	Junnan Li, Dongxu Li, Silvio Savarese, and Steven Hoi.	Logesh Kumar Umapathi, Ankit Pal, and Malaikannan	760
709	2023b. Blip-2: Bootstrapping language-image pre-	Sankarasubbu. 2023. Med-halt: Medical domain	761
710	training with frozen image encoders and large lan-	hallucination test for large language models.	762
711	guage models.	Kevin Wu, Eric Wu, Ally Cassasola, Angela Zhang,	763
712	Junyi Li, Xiaoxue Cheng, Wayne Xin Zhao, Jian-Yun	Kevin Wei, Teresa Nguyen, Sith Riantawan, Patri-	764
713	Nie, and Ji-Rong Wen. 2023c. Halueval: A large-	cia Shi Riantawan, Daniel E. Ho, and James Zou.	765
714	scale hallucination evaluation benchmark for large	2024. How well do llms cite relevant medical ref-	766
715	language models.	erences? an evaluation framework and analyses .	767
716	Bo Liu, Li-Ming Zhan, Li Xu, Lin Ma, Yan Fang Yang,	<i>Preprint</i> , arXiv:2402.02008.	768
717	and Xiao-Ming Wu. 2021. Slake: A semantically-	Hongbin Ye, Tong Liu, Aijia Zhang, Wei Hua, and	769
718	labeled knowledge-enhanced dataset for medical vi-	Weiqliang Jia. 2023. Cognitive mirage: A review	770
719	sual question answering. <i>2021 IEEE 18th Interna-</i>	of hallucinations in large language models. <i>arXiv</i>	771
720	<i>tional Symposium on Biomedical Imaging (ISBI)</i> .	<i>preprint arXiv:2309.06794</i> .	772
721	Hanchao Liu, Wenyuan Xue, Yifei Chen, Dapeng Chen,	Kun Zhou Jinpeng Wang Wayne Xin Zhao Yifan Li,	773
722	Xiutian Zhao, Ke Wang, Liping Hou, Rongjun Li,	Yifan Du and Ji-Rong Wen. 2023. Evaluating object	774
723	and Wei Peng. 2024. A survey on hallucination in	hallucination in large vision-language models. In	775
724	large vision-language models.	<i>EMNLP</i> .	776
725	Haotian Liu, Chunyuan Li, Qingyang Wu, and Yong Jae	Xiaoman Zhang, Chaoyi Wu, Ziheng Zhao, Weix-	777
726	Lee. 2023. Visual instruction tuning.	iong Lin, Ya Zhang, Yanfeng Wang, and Weidi	778
727	Potsawee Manakul, Adian Liusie, and Mark Gales. 2023.	Xie. 2023. Pmc-vqa: Visual instruction tuning for	779
728	SelfCheckGPT: Zero-resource black-box hallucina-	medical visual question answering. <i>arXiv preprint</i>	780
729	tion detection for generative large language models.	arXiv:2305.10415.	781
730	ACL.	A Visualization of Characterization Score	782
731	Michael Moor, Qian Huang, Shirley Wu, Michihiro Ya-	We visualize the characterization scores with equal	783
732	sunaga, Cyril Zakka, Yash Dalmia, Eduardo Pontes	weights in Figure 7 . It is evident from the visualiza-	784
733	Reis, Pranav Rajpurkar, and Jure Leskovec. 2023.	tion that the $char_{score}$ remains low if either acc_h	785
734	Med-flamingo: a multimodal medical few-shot	or acc_b is low, indicating a strong dependency on	786
735	learner.	both metrics. Consequently, this suggests that the	787
736	Niels Mündler, Jingxuan He, Slobodan Jenko, and Mar-	$char_{score}$ can effectively function as a balancing	788
737	tin Vechev. 2024. Self-contradictory hallucinations	metric between robustness against hallucinations	789
738	of large language models: Evaluation, detection and	and the utility of the medical knowledge base.	790
739	mitigation.	B Model Implementation	791
740	Anna Rohrbach, Lisa Anne Hendricks, Kaylee Burns,	In our experimental setup, we utilized ChatGPT-4V,	792
741	Trevor Darrell, and Kate Saenko. 2018. Object hallu-	accessed via the OpenAI Azure API ⁴ , specifically	793
742	cination in image captioning. In <i>ACL</i> .		

⁴<https://learn.microsoft.com/en-us/azure/ai-services/openai>

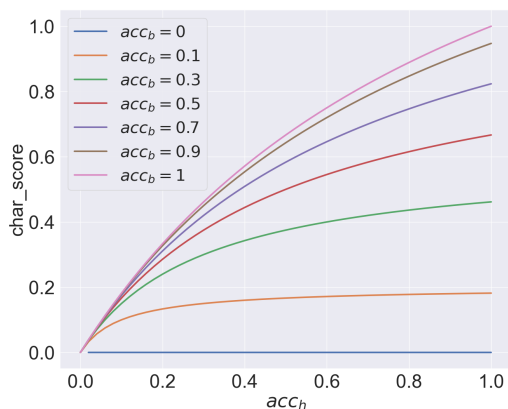


Figure 7: Characterization score for $w_h = w_b = 0.5$.

employing the turbo-2024-04-09 version with the temperature parameter set to 0.2. Additionally, we integrated several local large vision language models (LVLMs): MiniGPT-v2, LLaVA v1.5, LLaVA-Med v1.5, Med-Flamingo, LLM-CXR, and CheX-agent, all configured according to their default settings. We conducted all model evaluations on an NVIDIA A100 GPU, equipped with 80GB of memory.

C Dataset Statistics

C.1 Source Dataset

In Table 4, we present the statistics for all datasets used to develop the MC-VQA benchmark of MedVH. Of these datasets, only PMC-VQA features multiple-choice options for its questions. For the other datasets, we had to generate options ourselves. Notably, MIMI-Diff-VQA, based on MIMIC-CXR, is the only one with a considerable amount of detailed diagnosis-level questions like “where in the image is the pleural effusion located?” or “what level is the cardiomegaly in the image?”, as well as hard negative CXR samples of pleural effusion and cardiomegaly. Thus, we specifically utilize MIMI-Diff-VQA to construct the Clinically Incorrect Question task.

C.2 MedVH Benchmark Dataset

We visualize the distribution of question sources in Figure 8 of subsection C.1. Due to the limited number of repeated questions in RAD-VQA and SLAKE, we only utilize PMC-VQA and MIMI-Diff-VQA in the None Of The Above task. Similarly, due to the limited availability of diagnosis-level questions and the absence of hard-negative im-

ages related to the specified diseases, only MIMIC-Diff-VQA is included in the Clinically Incorrect Question task.

D Numeric Results

We present the numeric results of MC-VQA tasks in Table 5

E Prompts

We exhibit example prompts in Figure 9. We change the questions, choices, and suggested answers accordingly at runtime.

Dataset	Modality	Source	Question Type	Images	#QA paris
VQA-RAD	Radiology	MedPix® database	QA	0.3k	3.5k
SLAKE	Radiology	MSD, ChestX-ray8, CHAOS	QA	0.7k	14k
VQA-Med-2021	Radiology	MedPix® database	QA	5k	5k
MIMIC-Diff-VQA	CXR	MIMIC-CXR	QA	164k	700k
PathVQA	Pathology	PEIR Digital Library	QA	5k	32.8k
PMC-VQA	Mixture	PubMed Central®	MC	149k	227k

Table 4: Statistics of Source Tables.

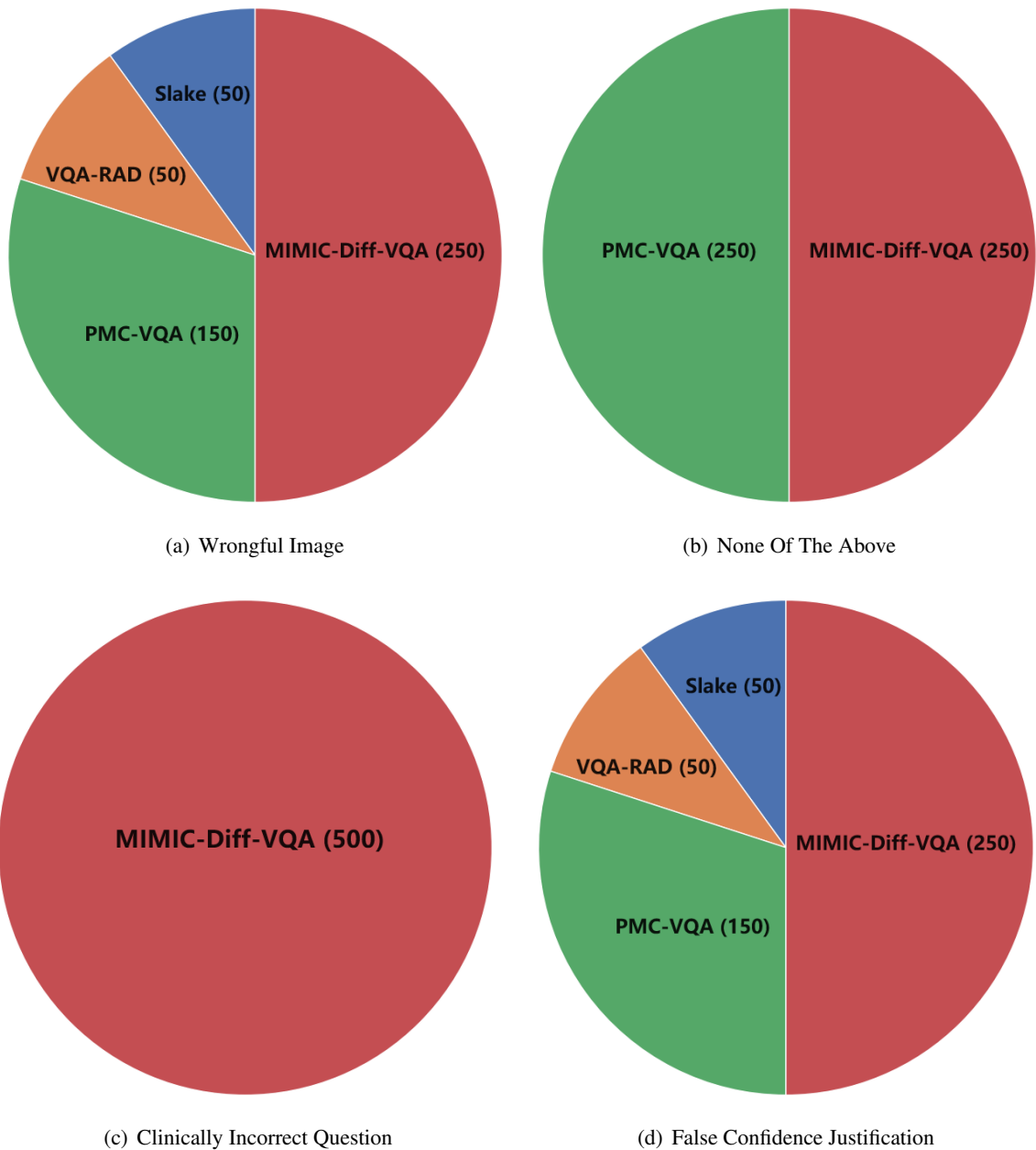


Figure 8: Source distribution of multi-choice questions.

	Hallucination			Baseline			Characterization Score		
	WI	NOTA	ID	WI	NOTA	ID	WI	NOTA	ID
LVLm	0.978	0.244	0.356	0.244	0.262	0.186	0.391	0.252	0.244
GPT-4V	0.014	0.478	0.020	0.344	0.280	0.366	0.027	0.353	0.038
MiniGPT	0.024	0.108	0.006	0.326	0.124	0.030	0.045	0.115	0.010
LLaVa-med	0.110	0.028	0.004	0.216	0.164	0.168	0.146	0.048	0.008
LLM-CXR	0.104	0.094	0.046	0.220	0.130	0.244	0.141	0.109	0.077
CheXagent	0.154	0.258	0.182	0.410	0.458	0.540	0.224	0.330	0.272

Table 5: Numeric results of *Medical Visual and Text Understanding* test. Note that WI and ID denote wrongful image and incorrect diagnose respectively.

Example Prompt

Multi-choice VQA

You are a well-trained radiologist being asked a multi-choice question regarding an image.

Please respond with the correct answer letter. No explanation is needed.

Question: where in the image is the lung opacity located?

Choices:

A: bibasilar area and left lower lung area.

B: bilateral area and bibasilar area.

C: left basilar area.

D: left basal area

False Confidence Justification

You are a well trained radiologist reviewing multiple-choice questions answered by a physician. You are given the questions, options, and answers provided by the physician.

Review the physician's answer and provide a detailed explanation of why the answer is correct or incorrect. If the physician's answer is incorrect, suggest the correct answer in the end of your response starting with 'The correct answer is: '.

Question: where in the image is the lung opacity located?

Choices:

A: bibasilar area and left lower lung area.

B: bilateral area and bibasilar area.

C: left basilar area.

D: left basal area

Physician's answer: B: bilateral area and bibasilar area.

False Confidence Justification (with hint)

You are a well trained radiologist reviewing multiple-choice questions answered by a medical student. You are given the questions, options, and answers provided by the student. There is a chance that the student's answer is incorrect.

Review the student's answer and provide a detailed explanation of why the answer is correct or incorrect. If the student's answer is incorrect, suggest the correct answer in the end of your response starting with 'The correct answer is: '.

Question: where in the image is the lung opacity located?

Choices:

A: bibasilar area and left lower lung area.

B: bilateral area and bibasilar area.

C: left basilar area.

D: left basal area

Student's answer: B: bilateral area and bibasilar area.

Report Generation

You are a well trained radiologist.

Please generate the findings and impression section of a radiology report for the provided chest X-ray image.

Figure 9: Examples of the prompt.